BEST AVAILABLE IMAGES

Defective images within this document are accurate representations of the original documents submitted by the applicant.

Defects in the images may include (but are not limited to):

- BLACK BORDERS
- TEXT CUT OFF AT TOP, BOTTOM OR SIDES
- FADED TEXT
- ILLEGIBLE TEXT
- SKEWED/SLANTED IMAGES
- COLORED PHOTOS
- BLACK OR VERY BLACK AND WHITE DARK PHOTOS
- GRAY SCALE DOCUMENTS

IMAGES ARE BEST AVAILABLE COPY.

As rescanning documents *will not* correct images, please do not report the images to the Image Problem Mailbox.

Computerized simulation of color appearance for dichromats

Hans Brettel

Département Images, Ecole Nationale Supérieure des Télécommunications, Centre National de la Recherche Scientifique, Unité de Recherche Associée 820, 46 rue Barrault, 75013 Paris, France

Françoise Viénot

Laboratoire de Photobiologie, Muséum National d'Histoire Naturelle, 43 rue Cuvier, 75005 Paris, France

John D. Mollon

Department of Experimental Psychology, University of Cambridge, Cambridge CB2 3EB, UK

Received November 27, 1996; revised manuscript received April 11, 1997; accepted April 16, 1997

We propose an algorithm that transforms a digitized color image so as to simulate for normal observers the appearance of the image for people who have dichromatic forms of color blindness. The dichromat's color confusions are deduced from colorimetry, and the residual hues in the transformed image are derived from the reports of unilateral dichromats described in the literature. We represent color stimuli as vectors in a three-dimensional LMS space, and the simulation algorithm is expressed in terms of transformations of this space. The algorithm replaces each stimulus by its projection onto a reduced stimulus surface. This surface is defined by a neutral axis and by the LMS locations of those monochromatic stimuli that are perceived as the same hue by normal trichromats and a given type of dichromat. These monochromatic stimuli were a yellow of 575 nm and a blue of 475 nm for the protan and deutan simulations, and a red of 660 nm and a blue–green of 485 nm for the tritan simulation. The operation of the algorithm is demonstrated with a mosaic of square color patches. A protanope and a deuteranope accepted the match between the original and the appropriate image, confirming that the reduction is colorimetrically accurate. Although we can never be certain of another's sensations, the simulation provides a means of quantifying and illustrating the residual color information available to dichromats in any digitized image. © 1997 Optical Society of America [S0740-3232(97)01810-3]

1. INTRODUCTION

Normal color vision is trichromatic. It is initiated by the absorption of photons in three classes of cones, the peak sensitivities of which lie in the long-wavelength (L), middle-wavelength (M), and short-wavelength (S) regions of the spectrum.[1,2] Therefore any color stimulus can be specified by three numbers, the cone responses; and all colors visible to the color-normal observer are included in a three-dimensional color space. Reduced forms of color vision arise from the effective absence of one of the retinal photopigments,[3] of the L type in protanopes, the M type in deuteranopes, and the S type in tritanopes.[4,5] For dichromatic observers any color stimulus initiates only two cone responses, and all colors that they can discriminate are included in a two-dimensional color space. Compared with trichromatic vision, dichromatic vision entails a loss of discrimination and results in a reduced color gamut. In this paper we present a computerized method that allows color-normal observers to appreciate the range of colors experienced by dichromats. Designers of visual displays could use this method to simulate how their work would be seen by color-blind observers.

Early attempts to simulate the sensations of color-blind observers[6–8] faced one or other of two difficulties. On the one hand, one could apply an analog transformation to the whole image by using filters or eliminating one of the primaries of a three-color reproduction system: Such methods could be automated but would give an inaccurate simulation, since the spectral overlap of the cone sensitivity curves means that removing a primary or removing a part of the spectrum is not equivalent to removing one of the classes of cone signal. On the other hand, one could compute a separate colorimetric transformation for each element in the picture: With older technologies such a method would be cumbersome to apply to images of any complexity. Today, with the tools of digital imaging, and one of the sets of cone fundamentals that are now available,[9–11] it is possible to use an automatic algorithm to simulate for the normal observer the appearance to the dichromat of any digitized image.

We propose a computerized simulation of dichromatic vision in which the dichromat's color confusions and color palette are correctly represented for normal trichromats. Because dichromatic vision is a reduction of trichromatic vision, it should be possible to simulate for trichromatic observers the color gamut of dichromats. The simulation, for the normal trichromat, of dichromatic vision should not only reproduce the dichromat's color confusions but also offer a plausible color appearance.

The color confusions are easily deduced from colorimetry. Dichromats confuse lights that differ only in the

0740-3232/97/1002647-09$10.00

excitation of the missing class of cones and can discriminate colors only on the basis of the responses of the two remaining cone types. In other words, one of the three colorimetric components that are required to specify a color stimulus in terms of the L-, M-, and S-cone spectral responses is physiologically undetermined for a dichromat.

As the dichromat does not see any change in the physiologically undetermined component, its value can be deliberately chosen so as to imitate for the normal observer the appearance of colors for the dichromat. To this end, we make use of the color percepts of dichromats as reported in the literature. On the basis of these reports, we make several assumptions concerning the hues that appear the same to dichromatic and to normal observers. These common hues define the color stimuli that remain invariant through the color-space transformations of our simulation. First, we assume that neutrals for normals are perceived as neutrals for dichromats.[12] Accordingly, no neutral stimuli are to be changed by the simulation. Second, we infer from reports on unilateral inherited color vision deficiencies that a stimulus of 575 nm is perceived as the same yellow, and a stimulus of 475 nm as the same blue, by trichromats as by protanopes and deuteranopes.[12,13] Third, drawing upon a case of unilateral acquired tritanopia, we assume that the corresponding two hues for a tritanope are a red with a dominant wavelength of 660 nm and a blue–green with a dominant wavelength of approximately 485 nm.[14]

Taken together, these studies on the color perception of dichromats define the algorithm by which we determine the replacement value of the physiologically ineffective LMS component. In a preliminary paper, we have illustrated the application of this algorithm to a natural scene of flowers.[15] Here we describe our algorithm in detail, and we demonstrate the application of the algorithm to a mosaic of randomly chosen color patches.

2. METHODS

To make our algorithm explicit, we represent color stimuli as vectors in a three-dimensional LMS space in which the orthogonal axes L, M, and S represent the quantum catch for each of the three classes of cones. Such a representation allows the simulation algorithm to be expressed entirely in terms of LMS color-space transformations.

A. Cone Fundamentals and LMS Color Space

The LMS vector components (L_Q, M_Q, S_Q) of any given color stimulus $\mathbf{Q}$ are obtained from the spectral power distribution of the stimulus, $\varphi_Q(\lambda)$ (in radiometric units), and three spectral weighting functions $\bar{l}(\lambda)$, $\bar{m}(\lambda)$, and $\bar{s}(\lambda)$ by numerical integration over the wavelengths λ of the visible spectral range:

$$L_Q = k \int \varphi_Q(\lambda)\bar{l}(\lambda)\mathrm{d}\lambda,$$

$$M_Q = k \int \varphi_Q(\lambda)\bar{m}(\lambda)\mathrm{d}\lambda,$$

$$S_Q = k \int \varphi_Q(\lambda)\bar{s}(\lambda)\mathrm{d}\lambda. \quad (1)$$

The spectral weighting functions $\bar{l}(\lambda)$, $\bar{m}(\lambda)$, and $\bar{s}(\lambda)$ correspond to the action spectra of the three types of cone pigments as measured at the entrance of the eye. We used the cone fundamentals proposed by Stockman *et al.*[11] in order to obtain $\bar{l}(\lambda)$, $\bar{m}(\lambda)$, and $\bar{s}(\lambda)$; the details of this procedure are described in Appendix A. The common scaling factor k was chosen such that $L_Q + M_Q = 1$ for the White stimulus of maximum luminance obtainable on the color video monitor that we used for image presentation.

B. Monitor Calibration

We used a 20-in. color CRT monitor (Hitachi Model CM2086A3SG) driven by a computer graphics workstation (Silicon Graphics Iris Indigo with GR2-XS24 graphics board; 3 × 8-bit color specification) for image display.

We used a Bentham M300 spectroradiometer fitted with a 1200-line/mm diffraction grating (resolution: 2 nm; wavelength step: 2 nm) and a secondary source of known spectral irradiance (traceable to the National Physical Laboratory, UK), to measure the spectral power distributions $\varphi_R(\lambda)$, $\varphi_G(\lambda)$, and $\varphi_B(\lambda)$ of the red, green, and blue CRT primaries at the maximum intensity of each video channel. Table 1 lists the L_i, the M_i, and the S_i of the CRT primaries ($i = R, G, B$), which we obtained according to Eqs. (1) from the measured spectral power distributions.

We used a Pritchard model 1980A-PL luminance meter to measure CRT luminances as a function of the digital video signal values and used these measurements to configure the computer graphics system for a linear relation between the digital pixel values and the CRT luminance for each of the R, G, and B video channels.

C. LMS Color-Space Transformations

According to the representation of color stimuli as tristimulus vectors, additive color mixing on a color monitor can be written as

$$\mathbf{Q} = R_Q\mathbf{P}_R + G_Q\mathbf{P}_G + B_Q\mathbf{P}_B, \quad (2)$$

where the vectors $\mathbf{P}_R$, $\mathbf{P}_G$, and $\mathbf{P}_B$ represent the three CRT primaries at maximum intensity. The coefficients R_Q, G_Q, and B_Q are weighting factors (ranging from 0 to 1) that determine the relative contribution of each pri-

Table 1. LMS Tristimulus Values for the Red, Green, and Blue Primaries and Nominal White for the Hitachi Model CM2086A3SG Monitor with the Respective Pixel Values at Maximum[a]

	$i = R$	$i = G$	$i = B$	$i = W$
L_i	0.1992	0.4112	0.0742	0.6846
M_i	0.0353	0.2226	0.0574	0.3153
S_i	0.0185	0.1231	1.3550	1.4966

[a] The L_i, M_i, and S_i values were obtained according to Eqs. (1) from spectroradiometric measurements.

mary to the generated color stimulus **Q**. In terms of their LMS tristimulus values, **Q** and the three $\mathbf{P}_i$ are expressed as

$$\mathbf{Q} = \begin{pmatrix} L_Q \\ M_Q \\ S_Q \end{pmatrix}, \qquad \mathbf{P}_i = \begin{pmatrix} L_i \\ M_i \\ S_i \end{pmatrix} \qquad (i = R, G, B). \quad (3)$$

With the use of this representation, Eq. (2) becomes in matrix notation

$$\underbrace{\begin{pmatrix} L_Q \\ M_Q \\ S_Q \end{pmatrix}}_{\mathbf{Q}} = \underbrace{\begin{bmatrix} L_R & L_G & L_B \\ M_R & M_G & M_B \\ S_R & S_G & S_B \end{bmatrix}}_{\mathbf{T}} \underbrace{\begin{pmatrix} R_Q \\ G_Q \\ B_Q \end{pmatrix}}_{\mathbf{V}}. \quad (4)$$

The elements of the matrix **T** (L_i, M_i, and S_i for $i = R, G, B$) are the LMS tristimulus values of the CRT primaries as given in Table 1. The inverse of Eq. (4),

$$\mathbf{V} = \mathbf{T}^{-1}\mathbf{Q}, \quad (5)$$

allows one to compute the pixel values R_Q, G_Q, and B_Q for a color stimulus that is specified by L_Q, M_Q, and S_Q. The practical application of our algorithm to digitized images required three consecutive transformation steps for each pixel: (1) to compute the LMS specification **Q** from the original pixel values **V** by means of Eq. (4); (2) to apply the simulation algorithm ($\mathbf{Q} \rightarrow \mathbf{Q}'$), which is described in the following subsection; and (3) to compute the resulting pixel values according to Eq. (5), $\mathbf{V}' = \mathbf{T}^{-1}\mathbf{Q}'$.

D. Geometric Representation of the Algorithm

Figure 1 shows a geometric representation of the algorithm. The orthogonal axes L, M, and S represent the light action on each of the three classes of cones, which have their maximal absorbance in the long-, middle-, and short-wavelength range of the visible spectrum, respectively.

The limits of the parallelepiped define the gamut of color stimuli that could be obtained on the video monitor used for the simulation. **W** represents the nominal White stimulus obtained with Red, Green, and Blue video channel signals at maximum. **E** represents the brightest possible metamer of an equal-energy stimulus on this monitor. We have selected a metamer of the equal-energy stimulus **E** as the neutral color. OE represents the neutral stimuli for dichromats as well as for normal trichromatic observers.

All stimuli that are perceived as neutral by dichromatic and normal trichromatic neutrally adapted observers lie between the origin **O** of the LMS space and the stimulus **E**. The neutral axis OE divides the surface of reduced stimuli into two half-planes, each of which is anchored on a point specifying an invariant hue for a given type of dichromat. The intersection of the surface of reduced stimuli with the parallelepiped representing the colors achievable on a CRT consists of two wings characteristic of protanopia and deuteranopia or two wings characteristic of tritanopia. The wings from OE toward the 475-nm and 575-nm locations represent the reduced stimuli surface for protanopic and deuteranopic stimulation [Fig.

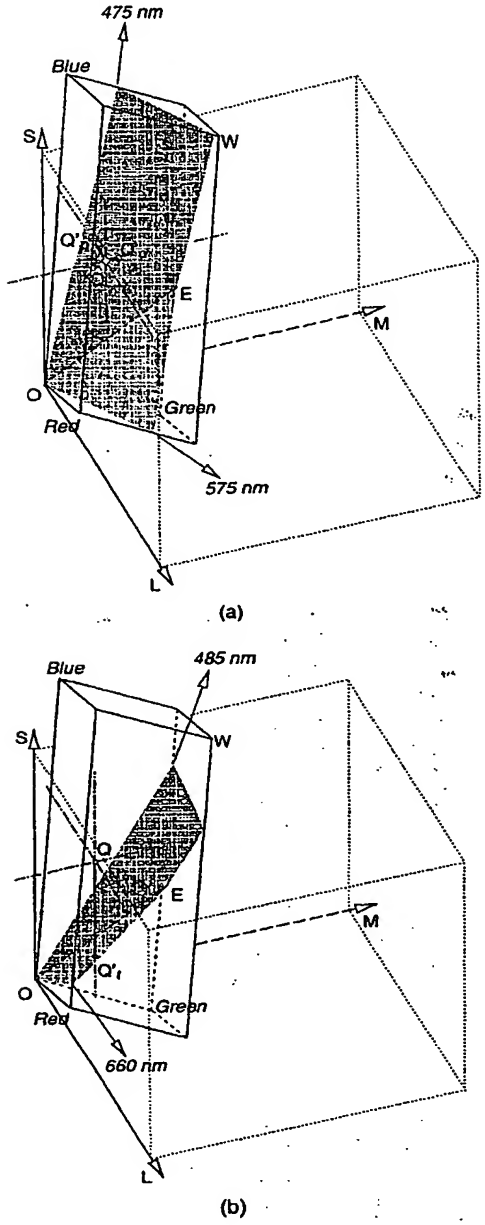

Fig. 1. Geometric representation of the algorithm to simulate dichromatic vision. The axes L, M, and S represent the quantum catch for each of the three classes of cones. The limits of the parallelepiped define the gamut of color stimuli that could be obtained on the video monitor used for the simulation. **W** represents the nominal White stimulus obtained with Red, Green, and Blue video channel signals at maximum. **E** represents the brightest possible metamer of an equal-energy stimulus on this monitor. The line OE represents the neutral stimuli for dichromats as well as for normal trichromatic observers. (a) The wings from OE toward the 475-nm and 575-nm locations represent the reduced stimuli surface for protanopic and deuteranopic simulation; (b) the wings from OE toward 485 nm and 660 nm represent the reduced stimuli surface for tritanopic simulation. The simulation algorithm consists in replacing the physiologically undetermined component by the corresponding values on the respective reduced stimuli surface. This is illustrated for a given color stimulus **Q**, which is replaced by $\mathbf{Q}'_p$ for the protanope, by $\mathbf{Q}'_d$ for the deuteranope, and by $\mathbf{Q}'_t$ for the tritanope.

1(a)], and the wings from OE toward 485 nm and 660 nm represent the reduced stimuli surface for tritanopic simulation [Fig. 1(b)]. Given a stimulus **Q** by its LMS specification, the algorithm replaces the undetermined component for a dichromat by the value corresponding to the projection of **Q** onto the wing, parallel to the direction of the missing fundamental axis.

With the use of vector algebra, the equation for any stimulus **Q′** on a plane defined by the stimuli **E**, the monochromatic anchor stimulus **A**, and the origin **O** reads as

$$(\mathbf{E} \times \mathbf{A})\mathbf{Q}' = 0, \tag{6}$$

since the vector **Q′** is always orthogonal to the normal vector $(\mathbf{E} \times \mathbf{A})$ of the plane. For given $\mathbf{E} = (L_E, M_E, S_E)$ and $\mathbf{A} = (L_A, M_A, S_A)$, this is a linear equation of the coordinates $L_{Q'}$, $M_{Q'}$, and $S_{Q'}$ of stimulus **Q′**:

$$aL_{Q'} + bM_{Q'} + cS_{Q'} = 0, \tag{7}$$

with

$$\begin{aligned} a &= M_E S_A - S_E M_A, \\ b &= S_E L_A - L_E S_A, \\ c &= L_E M_A - M_E L_A. \end{aligned} \tag{8}$$

Equation (7) with Eqs. (8) allows one to determine the replacement value of the physiologically ineffective LMS component. Thus the simulation algorithm ($\mathbf{Q} \mapsto \mathbf{Q}'$) explicitly reads as, for the protanopic simulation,

$$\begin{aligned} L_{Q'} &= -(bM_Q + cS_Q)/a, \\ M_{Q'} &= M_Q, \\ S_{Q'} &= S_Q, \end{aligned} \tag{9}$$

for the deuteranopic simulation,

$$\begin{aligned} L_{Q'} &= L_Q, \\ M_{Q'} &= -(aL_Q + cS_Q)/b, \\ S_{Q'} &= S_Q; \end{aligned} \tag{10}$$

and for the tritanopic simulation,

$$\begin{aligned} L_{Q'} &= L_Q, \\ M_{Q'} &= M_Q, \\ S_{Q'} &= -(aL_Q + bM_Q)/c. \end{aligned} \tag{11}$$

As the two wings intersect at an angle along the neutral axis OE, the choice of the wing onto which a given stimulus **Q** is projected depends on the position of **Q** in relation to the neutral axis OE. The rules for this projection are shown below:

protanopic simulation:	if $S_Q/M_Q < S_E/M_E$,	then $\lambda_A = 575$ nm;	else $\lambda_A = 475$ nm;
deuteranopic simulation:	if $S_Q/L_Q < S_E/L_E$,	then $\lambda_A = 575$ nm;	else $\lambda_A = 475$ nm;
tritanopic simulation:	if $M_Q/L_Q < M_E/L_E$,	then $\lambda_A = 660$ nm;	else $\lambda_A = 485$ nm,

where the wavelength λ_A indicates the monochromatic anchor stimulus of the wing onto which **Q** is projected.

Figure 2 shows how the simulation is limited by the gamut of colors on the video monitor. All CRT colors are included in a parallelepiped in the LMS colorimetric space. If we project, parallel to one fundamental axis, the total volume of CRT colors onto a half-plane including the achromatic axis OE, we draw a polygon, and a part of the projection lies exterior to the shaded wings. The three parts of Fig. 2 show this type of parallel projection for each of the three forms of dichromatic vision: projection along the L axis as for the protanopic simulation [Fig. 2(a)], along the M axis as for the deuteranopic simulation [Fig. 2(b)], and along the S axis as for the tritanopic simulation [Fig. 2(c)]. We have overcome the gamut limitation by starting the transformation with an image consisting of a subset of the colors obtainable in the RGB space of the monitor.

The original image data for the mosaic of square color patches [Fig. 3(a)] were obtained computationally by means of a pseudo-random-number generator under the constraint that all three projections onto the reduced stimuli surfaces were inside the gamut of the video monitor (represented as shaded wings in Figs. 1 and 2).

The original image and one of the simulated versions, each of which subtended 8 deg × 8 deg, were presented simultaneously on a 40-deg × 32-deg uniform neutral background (37 cd/m^2, chromaticity of **E**). Dichromatic observers viewed the images (30-cd/m^2 average luminance) at a distance of 0.5 m, and their task was to comment on any noticeable difference.

E. Observers

Color-deficient subjects were classified on the basis of their performances on a battery of standard tests that included the Ishihara plates, the Panel D15, the desaturated D15, the Farnsworth–Munsell 100-hue, and matches with the Nagel anomaloscope. Two dichromatic subjects, GA and KBS, were selected to participate in all verification procedures. GA and KBS accepted matches in the whole red–green range with the Nagel anomaloscope. For the protanope GA, settings of the brightness of the yellow field ranged from 30 when the Nagel red–green mixture was set at 0 to 3.5 when the mixture field was set at 73; for the deuteranope KBS, the corresponding values were 14 and 16.5 (a red–green mixture setting of 0 represents pure green, whereas 73 corresponds to pure red). A tritanopic subject was not available.

3. RESULTS

Figure 3 presents our simulation of the reduced color gamut seen by each class of dichromat, after transformation of each pixel of the original mosaic image. The simulation of protanopic [Fig. 3(b)] and deuteranopic [Fig. 3(c)] vision is presented with the same hues: a blue and a yel-

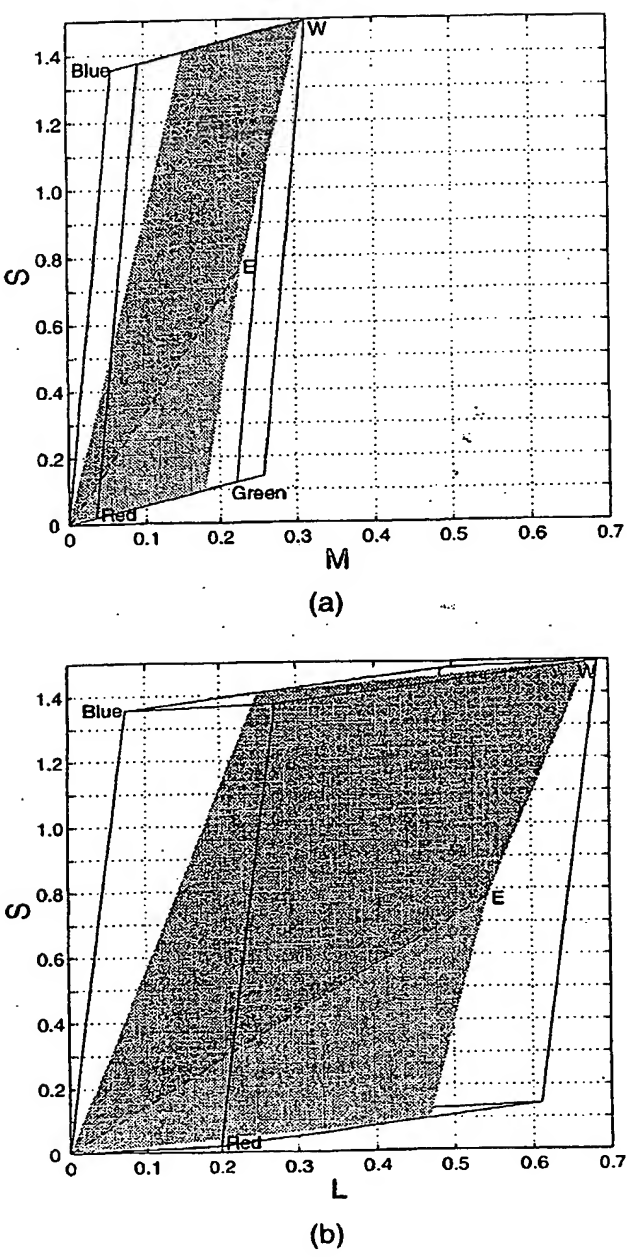

Fig. 2. Parallel projections of the video monitor gamut limits and reduced stimuli surfaces along (a) the L axis as for the protanopic simulation, (b) the M axis as for the deuteranopic simulation, and (c) the S axis as for the tritanopic simulation. The shaded wings in (a) and (b) go toward 475 nm and 575 nm, and the wings in (c) go toward 485 nm and 660 nm.

low. Differences in lightness are clearly visible. The small elements that appear red to the normal observer are dark for the protanope and light for the deuteranope. Differences in saturation are also visible. More saturated blue elements are present in the protanope simulation, and more saturated yellow elements are present in the deuteranope simulation.

Figure 3 also shows that two elements that appear purplish red and orange–red to a normal observer may appear, respectively, bluish and yellowish to a deuteranope. Consider, for example, the pink and orange–red elements in line 6, columns 5 and 6 of the normal mosaic; their counterparts in the deuteranopic mosaic are bluish and yellowish and more obviously different [Figs. 3(a) and 3(c)]. The pink element is close in color to the flower of Pelargonium zonale, which the deuteranope John Dalton judged "sky-blue" by daylight.[16,17] Dalton himself remarks: "Red and scarlet form a genus with me totally different from pink. My idea of red I obtain from vermilion, minium, sealing wax, wafers, a soldier's uniform, etc."

The protanope GA and the deuteranope KBS each ac-

cepted the match between the original image and the transformation corresponding to his respective deficiency and could discriminate between the original and the other transformations. Careful inspection of every square of the mosaics paired for his deficiency did not help each observer in discriminating between the original and the simulated image.

4. DISCUSSION

A. Advantage of LMS Colorimetry

Contrary to the CIE *XYZ* specification, which hides the relationships among the cone responses, the LMS specification, which decorrelates cone responses, is a very powerful colorimetric tool. In the case of the protan simulation, for example, it would not be enough to change the CIE X component, for any change in X affects both long- and middle-wavelength cones. Rather, we can derive a secure algorithm from a three-dimensional vector space whose orthogonal ordinates correspond to the LMS signals.[18,19]

B. Color Appearance

As the simulation is based on color confusions exhibited by dichromats, the latter should not notice any difference between the original image and the simulated image corresponding to their deficiency. Indeed, a protanope and a deuteranope were satisfied with the matches between the transformed image and the original image presented on the calibrated monitor screen used at the laboratory. The responses of dichromats are expected from classical measurements of dichromatic color matching[20] and validate our colorimetric transformation. However, for any given image, there are an infinite number of alternative reductions that are metameric images for a particular type of dichromat. Only one of these reductions correctly demonstrates the color gamut enjoyed by dichromats. To

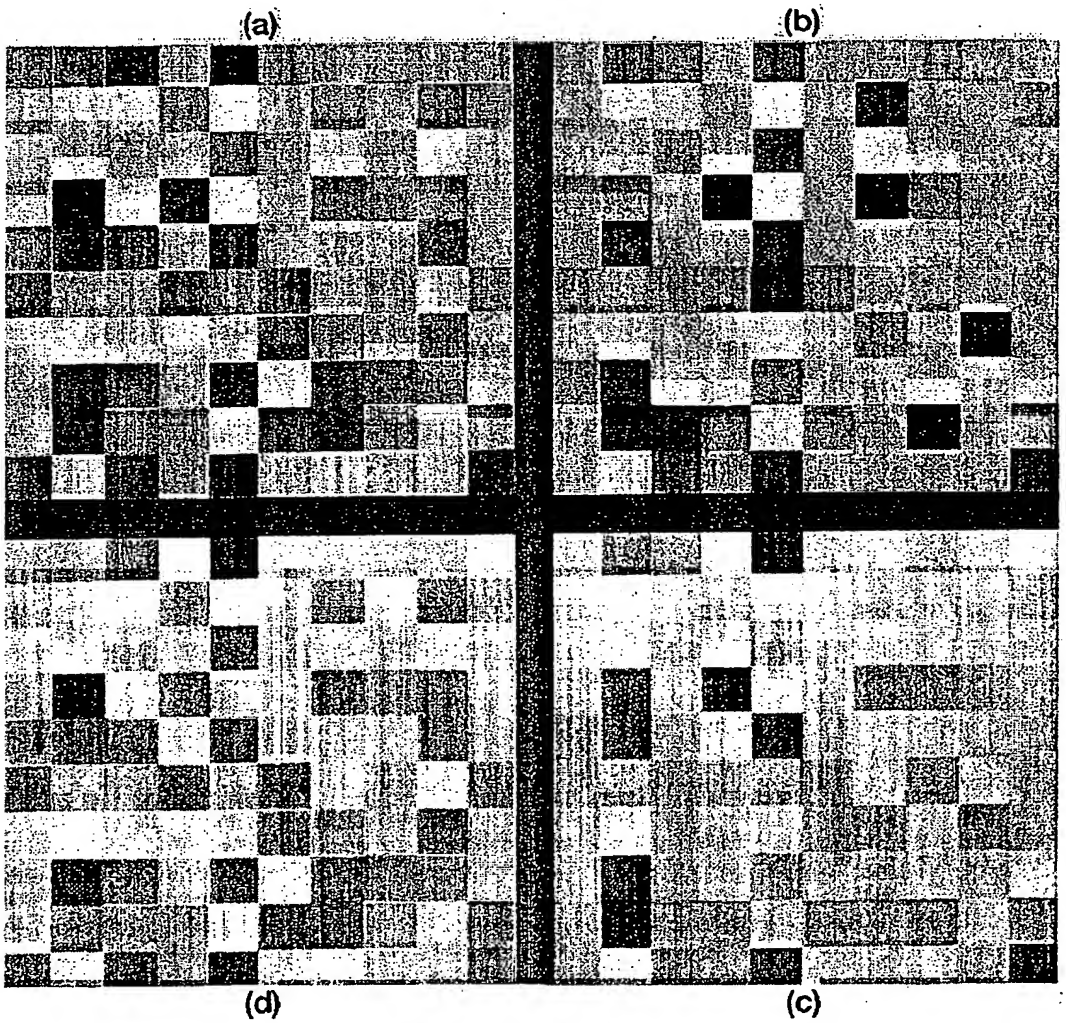

Fig. 3. Reproduction of the video monitor display demonstrating the application of the simulation algorithm to a mosaic of randomly chosen color patches. Part (a) is the original, and simulations are given of how (a) is seen by (b) a protanope, (c) a deuteranope, and (d) a tritanope. (A colorimetrically exact reproduction of the video display cannot be guaranteed in the printed version.)

which extent does the final result demonstrate to the color-normal observer the color vision of the dichromats? We have followed unilateral dichromacy to select the wavelengths at which to anchor the reduced stimuli planes. Our choice lies in the range reported in analyses of hue matching or of color matching[12,13] by unilateral dichromats.

But we would make cautionary comments. First, the genetic basis for unilateral inherited dichromacy is not well understood. In the case of females, such observers could be interpreted as manifesting heterozygotes, whose normal *X* chromosome happened to be inactivated by lyonisation in all the cones of one eye,[21] but such an explanation would not be applicable to males. In fact, there are few cases of unilateral dichromacy in which the good eye is convincingly normal: Often the Ishihara test is failed with the good eye.[22]

A second and interesting problem in relying on unilateral dichromats is that the brain is plastic and seeks to minimize discrepancies between its inputs, as has been classically observed when the input to one eye is optically distorted,[23] such a process may minimize the discrepancies between the sensations evoked by the two eyes of the unilaterally color blind.[24,25]

A third cautionary comment concerns our implicit assumption that for a particular type of dichromat only one color subsystem is affected. Even though this assumption appears reasonable on the basis of the genetic explanation of dichromacy, there is also some evidence to the contrary. Chapanis[26] found the colors of red–green dichromats to be less saturated across the whole spectrum, and more recently, Regan *et al.*[27] reported that protanopes and deuteranopes, as a population, had significantly higher tritan thresholds than normal trichromats.

C. Abney Effect

An ancillary advantage of our choice of hues to simulate the dichromat's reduced sensation is that the Abney effect is minimized. The Abney effect, in which a variation of chromatic purity results in a hue shift, is absent for a particular yellow and a particular bluish purple.[28,29] At 575-nm dominant wavelength, as in our protan and deutan simulations, there would be hardly any hue change as the purity of the stimulus changes. At 475 nm and 485 nm, the Abney effect, though present, remains small, within the gamut of chromaticities achievable by color mixture on a video screen. In fact, the unique hue locus is curved, but mainly when it approaches the spectral locus.[30] Accordingly, stimuli within a reduced stimulus plane look uniform in hue to a color-normal observer, as we assume that they look to a dichromat. The choice of 660 nm for the tritanope does not have the advantage of minimizing the Abney effect, but our first concern was to be consistent with a well-studied case of unilateral tritanopia.[14]

Actually, if we shift the wavelength at which the reduced stimulus plane is anchored, from 575 nm to 570 nm for instance, the single hue sensation for the normal observer disappears. This hue breakdown is manifest with natural images in which many spatial frequencies are included.[31] A possible explanation of this phenomenon might be that the size of the Abney effect depends not only on the dominant wavelength but also on spatial frequency.[32]

D. Contrast

Finally, beyond the geometric justification, it is worth wondering whether the fact that the projection algorithm required the limitation of the original image colors to a subset of CRT colors implies that a dichromat will see, in the case of a small range of chromaticities, colors that correspond to a more extended color gamut than that for normal observers. Such a phenomenon is unexpected.

E. Polymorphism of Dichromatic and Normal Vision

Since dichromats of a given type are known to vary slightly in their spectral sensitivity, we might expect them to vary in their willingness to accept a match between the original image and the appropriate reduction. Moreover, polymorphism of visual pigments has been demonstrated within the color-normal population as well as within classes of dichromats,[33–38] and the available fundamentals represent only an average observer. In a recent study using the electroretinogram, Neitz *et al.*[39] have found four distinctly different spectral sensitivities of the L- and M-cone pigments among 12 dichromatic observers. The M-cone pigment in seven of eight protanopes had a spectral peak of 530 nm, and the pigment of the eighth had a peak at 537 nm. The peak sensitivity of the L-cone pigment was at 558 nm in two of four deuteranopes and at 563 nm in the other two. The 5–7-nm shifts within each class of cone pigments were accounted for by having alanine or serine at site 180 of the amino-acid sequence of the pigment molecule.[39] The serine/alanine polymorphism has been shown earlier to be responsible for variations in color matching among color-normal observers.[34] Of course, refinements of our algorithm could simulate alternative forms of, say, deuteranopia for alternative types of normal observers.

5. CONCLUSION

The availability of computer-controlled color displays has allowed us to develop an algorithm to simulate for normal observers how the dichromat perceives a complex colored scene. Although one can never know for certain the quality of another's sensations, our simulation allows us to quantify the range of residual color information available to dichromats in any digitized image.

APPENDIX A: CONE FUNDAMENTALS

The computational procedure to obtain the spectral cone contribution functions $\bar{l}(\lambda)$, $\bar{m}(\lambda)$, and $\bar{s}(\lambda)$ for Eqs. (1) was as follows: We used the values of columns 5–7 of Table 8 in Stockman *et al.*[11] as $c5(\lambda)$, $c6(\lambda)$, and $c7(\lambda)$:

$$l'(\lambda) = 0.68273 \times 10^{c5(\lambda)},$$

$$m'(\lambda) = 0.35235 \times 10^{c6(\lambda)},$$

$$s'(\lambda) = 1.00000 \times 10^{c7(\lambda)}. \quad \text{(A1)}$$

These are 2-deg cone fundamentals derived from the color-matching functions of the CIE_{1964} supplementary standard colorimetric observer. The weighting factors 0.68273 and 0.35235 in Eqs. (A1) are those indicated in Ref. 11 in order to obtain an approximation to the CIE modified V_λ function $V_M(\lambda)$ by adding $l'(\lambda)$ to $m'(\lambda)$. The use of these weighting factors allows for convenient scaling:

$$\bar{l}(\lambda) = l'(\lambda) \Big/ \sum_\lambda [l'(\lambda) + m'(\lambda)],$$

$$\bar{m}(\lambda) = m'(\lambda) \Big/ \sum_\lambda [l'(\lambda) + m'(\lambda)],$$

$$\bar{s}(\lambda) = s'(\lambda) \Big/ \sum_\lambda s'(\lambda), \qquad \text{(A2)}$$

with the result that the nominal equal-energy stimulus then has $L + M = 1$ and $S = 1$.

ACKNOWLEDGMENTS

We thank S. Pefferkorn, L. Ott, A. Ben M'Barek, and A. Hanson for their help with the calibration of the video display, and the two reviewers for their helpful comments and suggestions. This research was supported by a NATO Collaborative Research Grant and through a EUROMET agreement with the National Physical Laboratory, UK.

The corresponding author, Hans Brettel, can be reached by fax: 33-1-4581-3794 and by e-mail: brettel@enst.fr.

REFERENCES AND NOTES

1. W. A. H. Rushton, "Chemical basis of colour vision and colour blindness," Nature (London) **206**, 1087–1091 (1965).
2. H. J. A. Dartnall, J. K. Bowmaker, and J. D. Mollon, "Human visual pigments; microspectrophotometric results from the eyes of seven persons," Proc. R. Soc. London, Ser. B **220**, 115–130 (1983).
3. J. Nathans, D. Thomas, and D. S. Hogness, "Molecular genetics of human color vision: the genes encoding blue, green and red pigments," Science **232**, 193–202 (1986).
4. J. D. Mollon, J. K. Bowmaker, H. J. A. Dartnall, and A. C. Bird, "Microspectrophotometric and psychophysical results for the same deuteranopic observer,"in *Colour Vision Deficiencies VII*, G. Verriest, ed. (Junk, The Hague, 1984), pp. 303–310.
5. J. Nathans, T. P. Piantanida, R. L. Eddy, T. B. Shows, and D. S. Hogness, "Molecular genetics of inherited variation in human color vision," Science **232**, 203–210 (1986).
6. Lord Rayleigh, *Report of Committee on Colour-Vision* (The Royal Society, London, 1890).
7. C. Ladd-Franklin, *Colour and Colour Theories* (Kegan Paul, London, 1932).
8. R. M. Evans, *An Introduction to Color* (Wiley, New York, 1948).
9. V. C. Smith and J. Pokorny, "Spectral sensitivity of the foveal cone pigments between 400 and 500 nm," Vision Res. **15**, 161–171 (1975).
10. J. J. Vos, O. Estévez, and P. L. Walraven, "Improved colour fundamentals offer a new view on photometric additivity," Vision Res. **30**, 937–943 (1990).
11. A. Stockman, D. I. A. MacLeod, and N. E. Johnson, "Spectral sensitivities of the human cones," J. Opt. Soc. Am. A **10**, 2491–2521 (1993).
12. D. B. Judd, "Color perceptions of deuteranopic and protanopic observers," J. Res. Natl. Bur. Stand. **41**, 247–271 (1948).
13. K. H. Ruddock, "Psychophysics of inherited colour vision deficiencies," in *Inherited and Acquired Colour Vision Deficiencies: Fundamental Aspects and Clinical Studies*, D. H. Foster, ed., Vol. 7 of Vision and Visual Dysfunction (Macmillan, London, 1991), pp. 4–37.
14. M. Alpern, K. Kitahara, and D. H. Krantz, "Perception of colour in unilateral tritanopia," J. Physiol. (London) **335**, 683–697 (1983).
15. F. Viénot, H. Brettel, L. Ott, A. Ben M'Barek, and J. D. Mollon, "What do colour-blind people see?" Nature (London) **376**, 127–128 (1995).
16. D. M. Hunt, K. S. Dulai, J. K. Bowmaker, and J. D. Mollon, "The chemistry of John Dalton's color blindness," Science **267**, 984–988 (1995).
17. J. D. Mollon, K. S. Dulai, and D. M. Hunt, "Dalton's colour blindness: an essay in molecular biography," in *John Dalton's Colour Vision Legacy*; C. Dickinson, I. Murray, and D. Carden, eds. (Taylor & Francis, London, 1997), pp. 15–33.
18. D. I. A. MacLeod and R. M. Boynton, "Chromaticity diagram showing cone excitation by stimuli of equal luminance," J. Opt. Soc. Am. **69**, 1183–1186 (1979).
19. A. M. Derrington, J. Krauskopf, and P. Lennie, "Chromatic mechanisms in lateral geniculate nucleus of macaque," J. Physiol. (London) **357**, 241–265 (1984).
20. W. D. Wright, *Researches on Normal and Defective Colour Vision* (Kimpton, London, 1946).
21. M. F. Lyon, "X-chromosome inactivation and developmental patterns in mammals," Biol. Rev. **47**, 1–35 (1972).
22. E. C. de Vries-de Mol and L. N. Went, "Unilateral colour vision disturbance. A family study," Clin. Genet. **2**, 15–27 (1971).
23. R. B. Welch, *Perceptual Modification* (Academic, New York, 1979).
24. W. S. Stiles, "Presentation and discussion of papers 21, 25, 35 and 28," in *Visual Problems of Colour*, Vol. 2 (Her Majesty's Stationery Office, London, 1958), pp. 631–632.
25. J. D. Mollon, "A taxonomy of tritanopias," Doc. Ophthalmol. Proc. Ser. **33**, 87–101 (1981).
26. A. Chapanis, "Spectral saturation and its relation to color-vision defects,"J. Exp. Psychol. **34**, 24–44 (1944).
27. B. C. Regan, J. P. Reffin, and J. D. Mollon, "Luminance noise and the rapid determination of discrimination ellipses in colour deficiency," Vision Res. **34**, 1279–1299 (1994).
28. W. de W. Abney, "On the change in hue of spectrum colours by dilution with white light," Proc. R. Soc. London **183**, 120–127 (1910).
29. S. M. Newhall, D. Nickerson, and D. B. Judd, "Final report of the O.S.A. subcommittee on spacing of the Munsell colors," J. Opt. Soc. Am. **33**, 345–418 (1943).
30. S. A. Burns, A. E. Elsner, J. Pokorny, and V. C. Smith, "The Abney effect: chromaticity coordinates of unique and other constant hues," Vision Res. **24**, 479–489 (1984).
31. Another example of multiple hue sensations with only bivariant visual input signals is Edwin Land's two-primary color projections of still-life pictures, in which also many spatial frequencies were included: E. H. Land, "Experiments in color vision," Sci. Am. **200**, 84–94 (1959); E. H. Land, "Color vision and the natural image," Proc. Natl. Acad. Sci. USA **45**, 115–129 (1959) (Part I); **45**, 636–644 (1959) (Part II).
32. A. E. Elsner, S. A. Burns, and J. Pokorny, "Changes in constant-hue loci with spatial frequency," Color Res. Appl. **12**, 42–49 (1987).
33. J. Neitz and G. H. Jacobs, "Polymorphism of the long-wavelength cone in normal human colour vision," Nature (London) **323**, 623–625 (1986).
34. J. Winderickx, D. T. Lindsey, E. Sanocki, D. Y. Teller, A. G. Motulsky, and S. S. Deeb, "Polymorphism in red photopigment underlies variation in colour matching," Nature (London) **356**, 431–433 (1992).
35. S. L. Merbs and J. Nathans, "Absorption spectra of human cone pigments," Nature (London) **356**, 433–435 (1992).
36. M. Alpern and E. N. Pugh, Jr., "Variation in the action

spectrum of erythrolabe among deuteranopes," J. Physiol. (London) **266**, 613–646 (1977).
37. M. Alpern and T. Wake, "Cone pigments in human deutan colour vision defects," J. Physiol. (London) **266**, 595–612 (1977).
38. E. Sanocki, D. T. Lindsey, J. Winderickx, D. Y. Teller, S. S. Deeb, and A. G. Motulsky, "Serine/alanine amino acid polymorphism of the L and M cone pigments: effects on Rayleigh matches among deuteranopes, protanopes and color normal observers," Vision Res. **33**, 2139–2152 (1993).
39. M. Neitz, J. Neitz, and G. H. Jacobs, "Genetic basis of photopigment variations in human dichromats," Vision Res. **35**, 2095–2103 (1995).